

Combined Noninvasive Imaging and Luminometric Quantification of Luciferase-Labeled Human Prostate Tumors and Metastases

Nadia El Hilali, Nuria Rubio, Mercedes Martinez-Villacampa, and Jerónimo Blanco

Departamento de Patología Molecular y Terapéutica (NEH, NR, JB), Instituto de Investigaciones Biomédicas de Barcelona, Centro de Investigación y Desarrollo (CSIC), Barcelona, and Institut Català d'Oncologia (MM-V), Barcelona, Spain

SUMMARY: Noninvasive imaging should facilitate the analysis of changes in experimental tumors and metastases-expressing photoproteins and result in improved data consistency and experimental animal welfare. We analyzed quantitative aspects of noninvasive imaging of luciferase-labeled tumors by comparing the efficiency of noninvasive light detection with in vitro quantification of luciferase activity. An intensified charge coupled device video camera was used to noninvasively image luciferase-expressing human prostate tumors and metastases in nude mice, after ip inoculation of luciferin. Repeated imaging of anesthetized animals after intervening growth periods allowed monitoring of tumor and metastases development. Comparison of photon events recorded in tumor images with the number of relative light units from luminometric quantification of homogenates from the same tumors, revealed that the efficiency with which light escapes tumors is inversely related to tumor size and that intensified charge coupled device images alone are not sufficient for quantitative evaluation of tumor growth. However, a combined videometric and luminometric approach did allow quantification and was used to show the cytostatic effects of paclitaxel in three different human prostate tumors growing in nude mice. (*Lab Invest* 2002, 82:1563–1571).

A continuous noninvasive and quantitative tumor-monitoring system should produce gains in data consistency and savings in labor and animal resources, while at the same time, improve animal welfare. These are all desirable goals in cancer research and drug development.

Despite the apparent opacity of tissues, light can be used to probe physiologic functions and structures at depths of several millimeters (Benaron et al, 1997; Müller et al, 1993). Some successful approaches to noninvasive experimental tumor monitoring have been based on this property of light to depict in vivo fluorescent photons from the green fluorescent protein (Yang et al, 2000), introduced into tumor cells as traceable genetic markers, or from externally added fluorescent agents specifically activated at the tumor site by proteases (Weissleder et al, 1999).

Using a different approach, tumor images can be generated using photons that originate from cells tagged by induced expression of proteins that catalyze chemiluminescent reactions in the presence of an

exogenous substrate. Light from genetically manipulated cells expressing luciferase has been used in the past to noninvasively monitor gene activity in tissues of small animals, such as mammalian embryos (Matsumoto et al, 1994; Thompson et al, 1995), transgenic fish (Tamiya et al, 1990), *Drosophila* (Brandes et al, 1996), and plants (Kay, 1993; Millar et al, 1992, 1995). In larger animals such as mice, luciferase fused to the human immunodeficiency virus promoter has been used to report on the activity of the promoter transgene (Contag et al, 1997) and to study the clearance rate of a luciferase-expressing HeLa ascites tumor during antineoplastic drug treatment (Sweeney et al, 1999).

Although these are attractive strategies for monitoring tumor development, several problems should be solved before noninvasive imaging can be used as a reliable quantitative tool.

The principal problem is a consequence of the optical density of live tissues, which strongly absorb photons at the required wavelengths. In the case of fluorescence, excitatory photons must first reach the target and emitted photons must then travel to the detectors. Besides this, the normal fluorescence of many biologic components contributes to a high background that reduces sensitivity.

In the case of luminescence, photons usually emitted at low intensities need to travel only in one direction and reach the detectors to generate an image; however, this comparatively simpler situation is complicated by the requirement of substrate and

DOI: 10.1097/01.LAB.0000036877.36379.1F

Received July 23, 2002.

NEH and NR contributed equally to this work. This work was supported by grants from Fundación Ramon Areces, Fondo de Investigaciones Sanitarias (Grant 00/0850), and Fundació d'Investigació Sant Pau.

Address reprint requests to: Dr. J. Blanco, Instituto de Investigaciones Biomédicas de Barcelona, Departamento de Patología Molecular y Terapéutica, Jordi Girona, 18-26, 08034, Barcelona, Spain. E-mail: jbfpmr@cid.csic.es

oxygen reaching the tumor efficiently. To compound all these, photons from tumors and metastases located at varying depths within the organism must transverse irregularly shaped materials of nonuniform optical density and refractive index.

We have explored the quantitative aspects of using noninvasive imaging for monitoring tumor and metastasis development and evaluated the possibility of using noninvasive imaging as a quantitative analysis tool. Our strategy consisted in comparing the number of photon events recorded from tumors of different sizes imaged *in vivo* using a video camera with the number of photons produced by homogenates of the same tumors, measured using a luminometer as the standard reference for quantitative detection of light.

The luciferase from *Photinus pyralis* catalyzes the oxidation of luciferin, in the presence of ATP and oxygen, generating light photons and oxyluciferin (Campbell and Sala-Newby, 1996). Luciferase photons generated in tissue homogenates devoid of other endogenous light-generating reactions can be easily counted with a luminometer. These very sensitive photon-counting instruments typically respond linearly within a range of six decades and are ideally suited for quantitative evaluation of luciferase activity *in vitro*. We have previously used this strategy to quantitatively study the traffic of very small numbers of luciferase-labeled prostate tumor cells to mouse organs at very early stages of tumor spread (Rubio et al, 1998, 2000).

Prostate tumor cell lines such as PC-3 (Kaighn et al, 1979), DU 145 (Mickey et al, 1977), and LNCaP (Horszewicz et al, 1983) have been useful models to study metastatic behavior (Webber et al, 1997) and its dependence on implantation site (Pettaway et al, 1996; Stephenson et al, 1992; Thalmann et al, 1994; Yang et al, 1999). Metastatic prostate carcinoma, initially sensitive to androgen deprivation, frequently progresses past this stage, creating a therapy dilemma (Mahler and Denis, 1992). Paclitaxel, acting by stabilization of microtubule structures (Horwitz et al, 1982) and blocking cell division (De Brabander et al, 1982), has found application for treatment of many tumors; however, as a single agent, it is recognized to have only minimal effect on prostate carcinoma (Blagosklonny et al, 2000).

In this report we show that ip-inoculated luciferin, the luciferase substrate, readily reaches luciferase-expressing solid tumors and metastases in lymph nodes and lungs of living mice, allowing their imaging using a high-sensitivity low-light video camera enhanced with a intensified charge coupled device (ICCD). In addition, by comparing data from noninvasive imaging of tumors with the measurement of luciferase activity in tissue homogenates, it was also possible to evaluate the merits of noninvasive imaging and to quantify changes resulting from treatment with paclitaxel, in several human prostate tumors.

Results

Tumor Cell Detection Sensitivity

Prostate carcinoma PC-3.Sluc cells, labeled by stable integration of the firefly *Photinus pyralis* luciferase

gene, produced 0.997 relative light units (RLUs) per cell, determined by luminometry from the slope of cell number versus light emission regression plots.

To establish the ICCD video camera detection sensitivity, light photons from PC-3.Sluc cells, serially diluted in microtiter culture plates from 70 to 0 cells, were imaged after adding luciferin. As shown in Figure 1A, as few as four PC-3.Sluc cells per well could be detected; the regression plot of photon events, extracted from the recorded images, versus the number of cells in the wells was linear, with a slope of 736 photon events per cell.

Detection of Tumor Cells Inoculated in Mice Tissues

To account for the optical properties of live tissues, ICCD video images were generated from mice inoculated im or ip with known quantities of tumor cells. Composite pictures of luciferase photons emitted from tumors, superimposed on animal body images, are shown in Figure 1, B and C.

As few as 10^3 PC-3.Sluc cells could be detected at the im and ip inoculation sites. Regression plots show that from as few as 10^3 and up to 10^7 cells, there was a power-law relation between the number of recorded photon events and cell number, at both inoculation sites.

The exponents of the regression plots for the im- and ip-inoculated cells were 0.348 and 0.402, respectively. Because the relation between photon events and cell number is not linear, the detection sensitivity is a function of cell number. Thus, for 1000 cells, the sensitivities for light detection from the im and ip sites relative to that from the tissue culture plate were 0.18 and 0.08 times lower, respectively, whereas for 10,000 cells the relative detection sensitivities were 0.04 and 0.02 times lower, respectively.

Detection of Solid Tumors and Metastasis

Visualization of luciferase-labeled cells in solid tumors and metastases growing in mice is subject to restrictions imposed by the need of an adequate delivery of substrates, luciferin and oxygen, to the tumors, and by the optical density of the intervening tissues. Human prostate tumor cells PC-3.Sluc, expressing the luciferase gene, were inoculated im in the thighs and orthotopically in the prostate gland of nude mice. After the indicated growth times, primary tumors and metastases were imaged using the ICCD video camera, as described.

As shown in Figure 2A, 4-week-old PC-3.Sluc primary tumors generated in the thighs were easily observed, when tumor size was not sufficient for visual detection. After a further 2-week growth interval, a repeated image of the same animal showed the notable increase in tumor size (Fig. 2B). Whole body ventral images of mice bearing thigh tumors frequently showed small light spots in the pelvic area (Fig. 2, C and E), which examination at a closer range revealed to be composed of several distinct light emitting spots of roughly round shape (Fig. 2, D and F). Dissection of

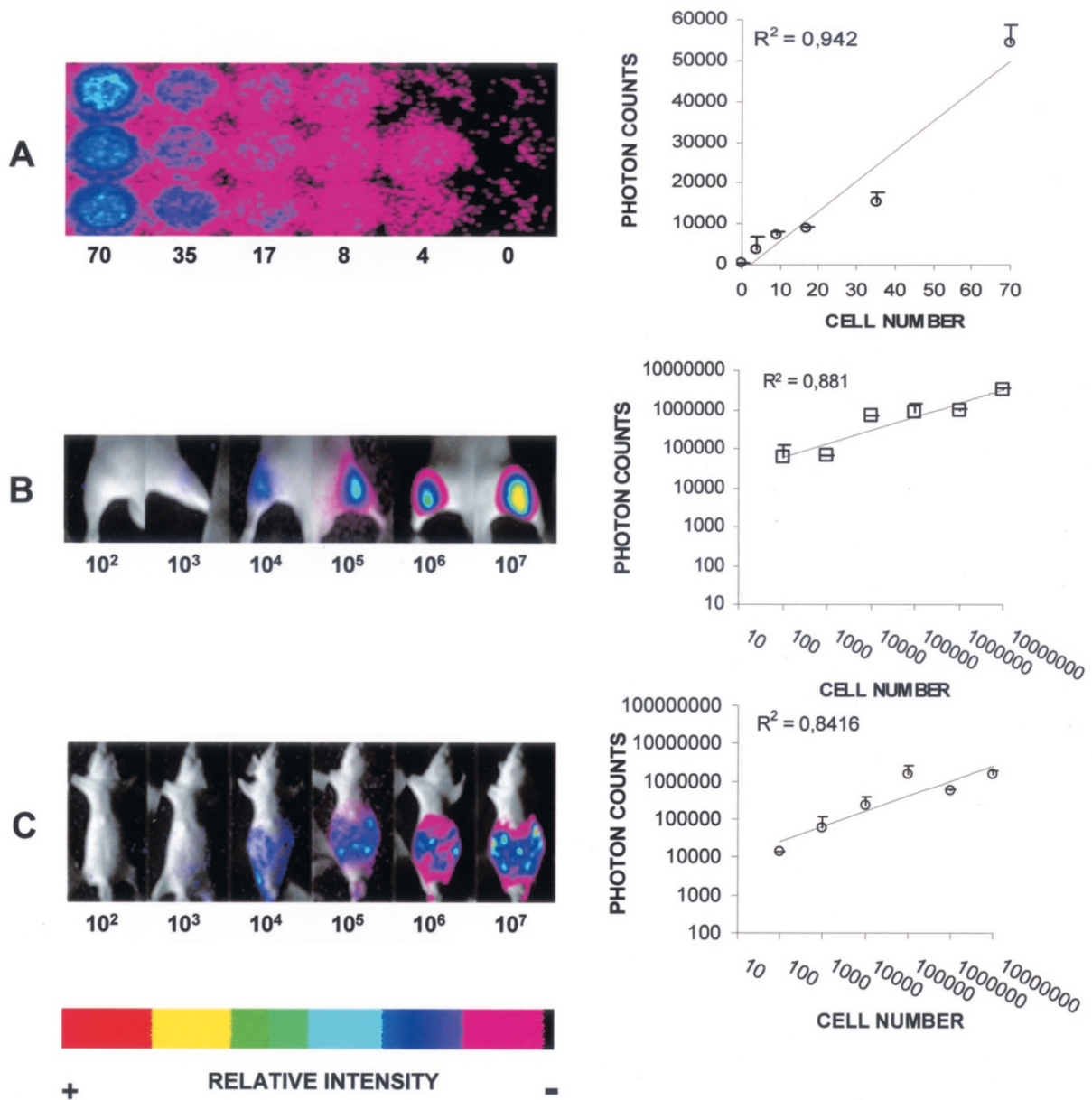


Figure 1.

Detection sensitivity for tumor cells in culture or inoculated in nude mice. Triplicate serial dilutions from 70 to 0 PC-3.Sluc cells were plated in 96-well microtiter tissue culture plates and imaged after adding luciferin (A). Serially diluted PC-3.Sluc cells were inoculated, in duplicate, in the thighs (B) or peritoneal cavity (C) of nude mice and directly imaged after addition of luciferin. A representative image of each cell inoculation is shown. Regression plots of the intensified charge coupled device–recorded photon events versus cell number are shown to the right of the corresponding images. Bars, standard deviation. Regression functions for (A): $Y = 736.33 \cdot X - 1580.9$; (B): $Y = 11731 \cdot X^{0.3485}$; (C): $Y = 3899.2 \cdot X^{0.4017}$.

mice on Fig. 2F, followed by luminometric analysis of tissue homogenates, showed that light emission originated from a grouping of large and small, 2 to 3 mm, lymph nodes colonized by a total of 24×10^6 tumor cell equivalents (TCEs).

Close-up video examination of the mice thoracic region (Fig. 2G) also revealed light emission in the shape of the lungs caused by abundant, 1.5×10^6 TCEs, as later shown by surgical removal and luminometric analysis of lung tissue. However, no tumor nodules could be observed.

One advantage of noninvasive imaging is monitoring of tumors growing in visually inaccessible sites.

PC-3.Sluc cells were orthotopically inoculated in the prostate gland of a nude mouse. After a 16-week growth period, ICCD video imaging of the ventral region revealed the presence of a tumor in the prostate region that was accompanied by a light spot in the thorax (Fig. 2H). Imaging of the surgically exposed thoracic cavity (Fig. 2I) revealed that light emission originated from a metastasized lymph node (Fig. 2J).

These results show that luciferase reaction substrates arrive at the tumors and allow repeated non-invasive observation of changes in their size. Despite a relatively low sensitivity, compared with luminometric procedures, tumors otherwise inaccessible to visual

PC-3.Sluc

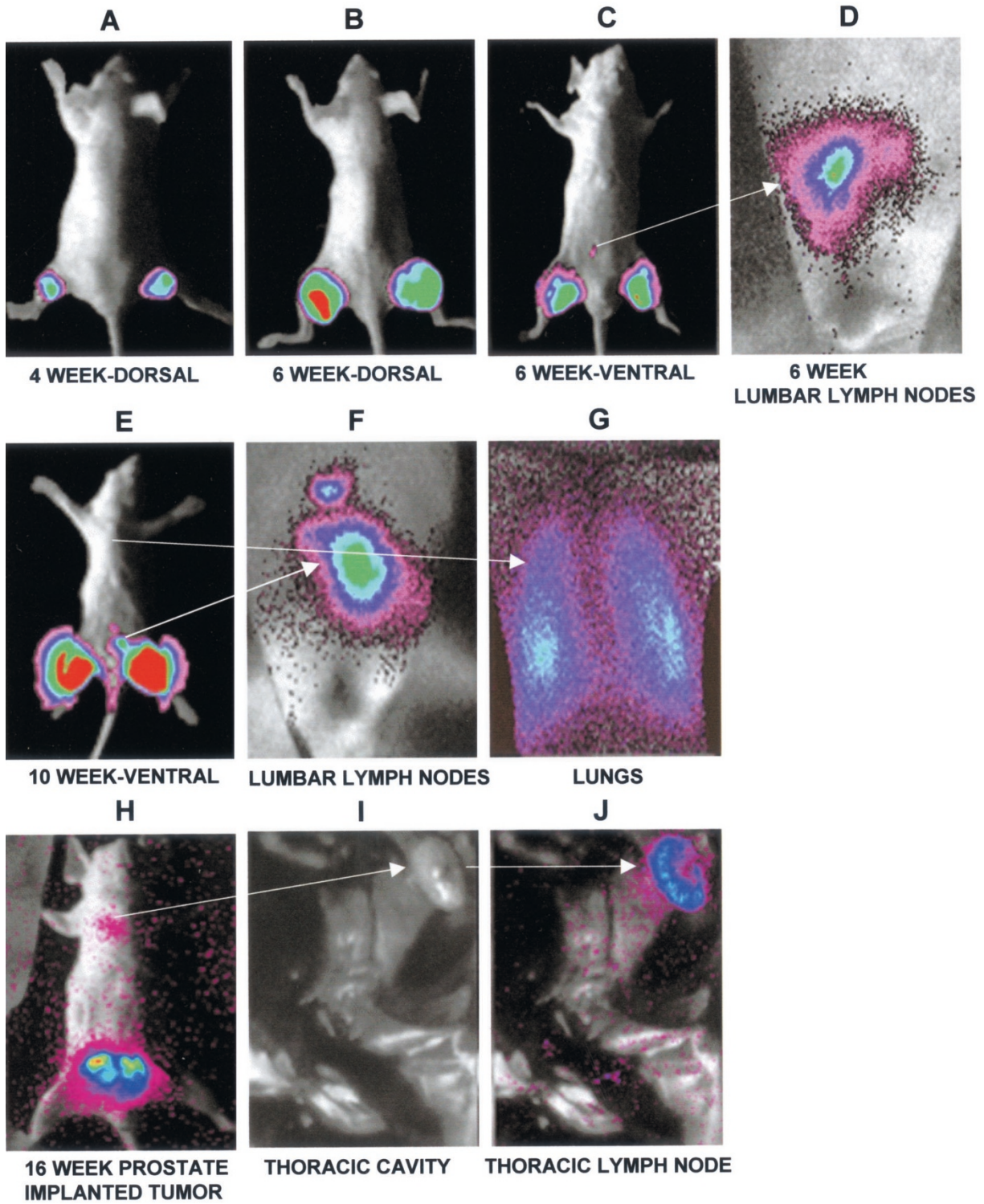


Figure 2.

Nude mice bearing PC-3.Sluc solid tumors in the thighs (A, B, C, and E) and in the prostate (H) and metastasis (D, F, G, and J) were visualized in anesthetized animals after ip inoculation of luciferin. A and B, Dorsal view of the same mouse at 4 and 6 weeks, respectively, after tumor inoculation. C, Ventral view of B. D, Close-up view of lumbar lymph node metastases (arrow). E, Ventral view of mouse with 10-week-old tumors in the thighs. Close-up ventral images showing lumbar lymph node (F) and lung metastases (G) (arrows). H, Prostate primary tumor, ventral view and close-up images of thoracic cavity showing internal organs (I) and light emission from a colonized lymph node (J) (arrows).

inspection because of their small size or hidden location could be monitored. In addition, dispersal of tumor cells, even if not forming tumor-like structures, as was the case in the lungs, was also detectable.

Monitoring of Antineoplastic Drug Effectiveness by the Videometric and Luminometric Procedures

Nude mice bearing prostate tumors PC-3.Sluc, DU 145.Sluc, and LNCaP.Sluc, having different growth rates and sensitivities to cytostatic agents, were either treated or not with 10 mg/kg paclitaxel and imaged before and after the treatment period (10 days). In these experiments an initial period of unrestricted tumor and metastasis development was allowed to mimic a clinical situation.

Figure 3A, left panel, shows nude mice in the initial state, with well-developed 30-day-old PC-3.Sluc primary tumors in both thighs. Incipient lumbar lymph node metastases were also visible in the pelvic region of both animals, but no lung involvement was apparent in either one. Figure 3A, right panel, shows the same animals after the 10-day treatment period. Control and treated mice showed a noticeable and equivalent increase in the light emitted by the primary tumors, indicating that paclitaxel had little or no effect. In the control mouse, a considerable development of the lumbar lymph node metastasis and clear colonization of the lungs by light-producing cells was evident. In contrast, the paclitaxel-treated mouse showed a decrease in light emission from the lumbar lymph nodes and no detectable light from the lungs.

Luminometric analysis of tissue homogenates showed the presence of a large number of light-emitting tumor cells in the lungs and lymph nodes of the untreated mouse (3.3×10^9 and 6.8×10^8 TCEs, respectively). The paclitaxel-treated mouse also contained a relatively small number of tumor cells in the lungs and lumbar lymph nodes (4×10^5 and 6.4×10^6 TCEs, respectively) that were not detectable by the ICCD camera. This detection limit, higher than that observed for directly inoculated cells, is possibly the result of higher optical density of intervening tissues.

Figure 3 (B, C, and D) compares the growth rate of PC-3.Sluc, DU 145.Sluc, and LNCaP.Sluc primary tumors in nude mice, either untreated or treated with paclitaxel. At the beginning of the treatment period, tumors were too small and could not be observed visually but generated a large number of photons, easily detectable by the ICCD camera. Visual comparison of tumor images from the onset of treatment (upper half panels) and from the end of the experimental trial (lower half panels) showed the evolution of the tumors during the test. Changes in tumor size, evaluated by counting photon events recorded in tumor images, are graphically depicted in the accompanying histograms at the right of each panel.

Paclitaxel had a different effect on each tumor type. PC-3 tumors were the most refractory, and tumor growth continued unimpaired during the treatment in all animals (Fig. 3B). In the case of DU 145 (Fig. 3C) and LNCaP tumors (Fig. 3D), paclitaxel treatment

resulted in an overall decrease in tumor size, but only in one case did a DU 145 tumor disappear to background level. Some tumors grew during the treatment. These results reproduce the known modest efficacy of this drug as a single therapy for prostate tumors and show the usefulness of noninvasive imaging to monitor behavior of individual tumors during therapy.

At the end of the treatment period, the animals were killed and homogenates of the primary tumors were luminometrically analyzed to determine total luciferase activity.

As indicated by the average for each tumor type and treatment status, control tumors were always clustered toward larger sizes and were higher RLU producers than treated tumors (Fig. 4). The significance of the difference in RLU production capacity between paclitaxel-treated and control tumors is an indicator of treatment efficacy. DU 145 ($p = 0.025$) and LNCaP ($p = 0.045$) were more responsive than PC-3 ($p = 0.197$) to paclitaxel, a result qualitatively consistent with that from tumor images.

Relation Between Photon Imaging and Luminometric Measurements

Figure 4 also shows the regression plot for the ratio of image-recorded photon events/RLUs from tumor homogenates, which is the *in vivo* detection efficiency, versus RLUs from tumor homogenates, a measurement of the number of tumor cells. The range of RLU production capacities for the LNCaP.Sluc, DU 145.Sluc, and PC-3.Sluc primary tumors analyzed (33 cases in all) was spread over 5 orders of magnitude, and the fitting function has a determination coefficient (R^2) of 0.7388.

The negative value for the fitting function slope shows that the *in vivo* detection efficiency using the video camera decreased with the increase in number of tumor cells and RLUs. For these tumors, the *in vivo* detection efficiency decreased by 3 orders of magnitude with a 4 orders of magnitude increase in tumor cell number.

The slopes of the fitting functions for the regression plots of the *in vivo* detection efficiency versus RLUs, for paclitaxel and control tumors independently, were equivalent. These results indicate that in the case of paclitaxel, it is tumor size and not the effect of treatment that determines the characteristic size-dependent change in light emission of the tumor. Most likely this drop in detection sensitivity is a consequence of tumor growth resulting in an increase in optical path and changes in the availability of substrates to the tumor core. This inevitable handicap in quantification by noninvasive video imaging could be corrected, in the present case and similar ones in which changes in light detection efficiency are tumor size dominated, by using a luminometer as an alternative size-independent measuring device, to standardize *in vivo* tumor image data.

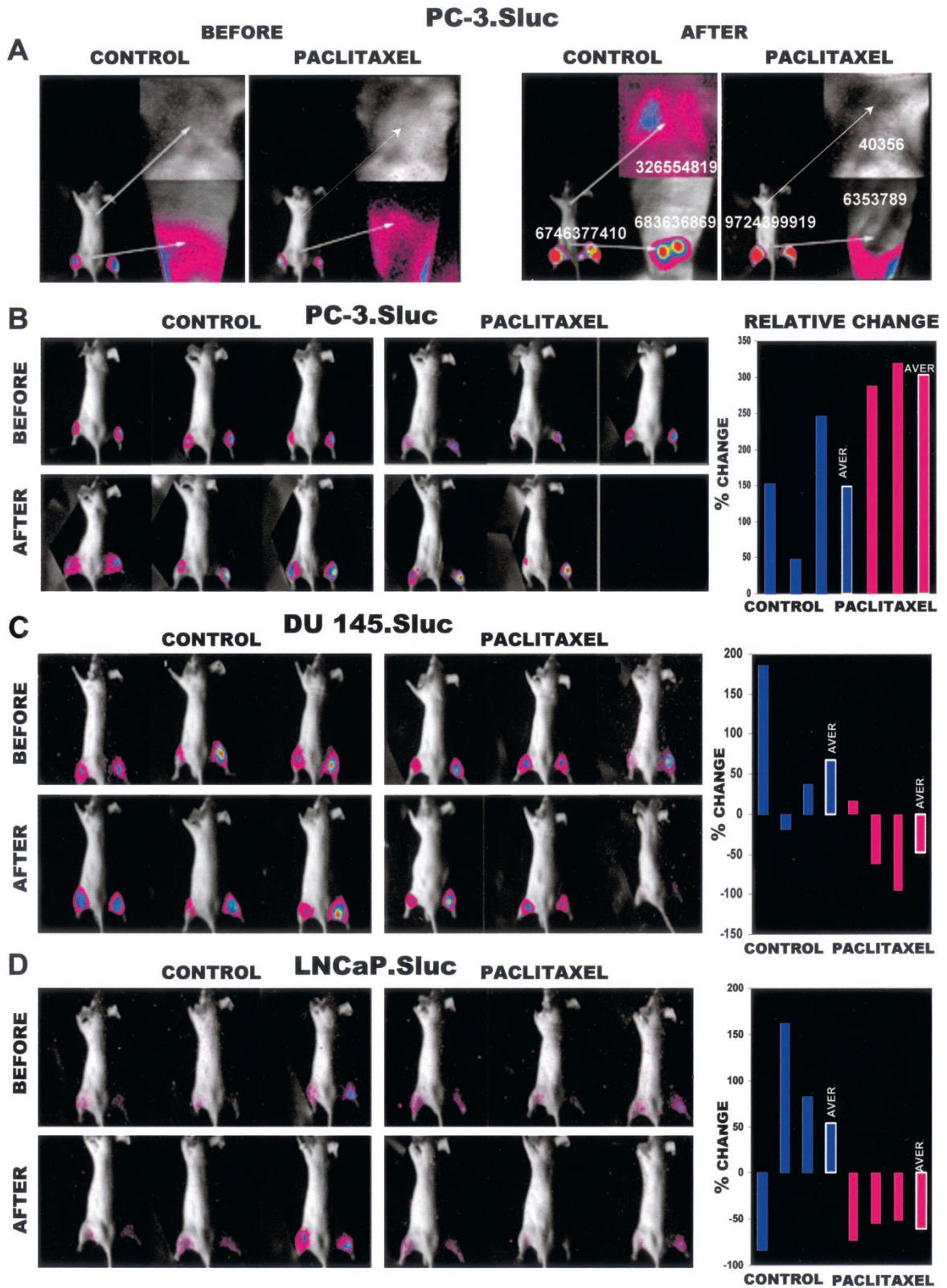


Figure 3.

Effect of paclitaxel on prostate tumor growth. A, Nude mice bearing 30-day-old PC-3.Sluc intramuscular tumors before (left) and after (right) 10 days of treatment with ip paclitaxel 10 mg/kg per day. The *arrows* indicate the position of developing metastasis. The *white overlaid numbers* show the relative light units (RLUs), measured in tissue homogenates of lungs and lumbar lymph nodes. Mice bearing 30-day-old PC-3.Sluc (B), DU 145.Sluc (C), and LNCaP.Sluc (D), intramuscular tumors before (upper half panels) and after (lower half panels) daily treatment with either 0.9% (w/v) NaCl solution (control) or paclitaxel 10 mg/kg for 10 days. The histograms at the right side of the panels show, for each mouse, the percent of change in recorded photon events from the tumors, relative to the start of the experiment. *White outlined bars* represent the group average.

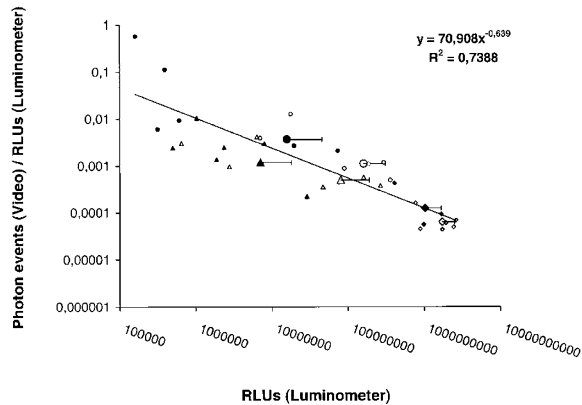


Figure 4.

Relation between efficiency of noninvasive light detection and primary tumor cell number. The ratio of photon events (video)/RLUs (luminometer) was plotted versus primary tumor RLUs (luminometer). DU 145.Sluc (\circ), LNCaP.Sluc (Δ), and PC-3.Sluc (\diamond). Controls, *open symbols*; paclitaxel, *solid symbols*; averages, *large symbols*. The regression function for all the tumors is indicated by the *solid line*. R^2 = determination coefficient. *Horizontal bars* = standard deviation.

Discussion

Noninvasive ICCD imaging of luciferase-labeled tumors in living animals is a convenient and more humane alternative to other procedures that require the death of large numbers of animals to monitor tumor and metastasis growth. Although ICCD cameras are very sensitive, constraints imposed by the optical properties of living tissues, including the tumors themselves, reduce sensitivity considerably relative to detection of tumor cells *in vitro*. Despite this, tumors either too small for direct visual detection or hidden in internal body locations, and therefore not detectable by direct inspection, were imaged and their development could be monitored. Small metastases to lymph nodes, ranging in the longest dimension from 2 to 3 mm, and diffuse colonization of the lungs were, for the first time, imaged by this noninvasive ICCD procedure. Noninvasive imaging and luminometric procedures were used to monitor the effectiveness of paclitaxel in the treatment of three different human prostate tumors covering a wide range of sizes. Both approaches produced equivalent qualitative results pointing to a modest and tumor-dependent efficacy of the drug. However, both procedures were not equivalent, and as tumor size increased, there was a proportional drop in the efficiency with which light could be detected by external video equipment, a quantification handicap that could be corrected by luminometric analysis and standardization using tumor homogenates.

There could be several phenomena that could, singly or in combination, account for this experimental result. Because Figure 4 depicts the relation between the number of tumor cells and the efficiency with which the video system records photons, in the absence of other factors, the graph should have been a horizontal line. However, tumor growth is not only accompanied by an increase in the number of cells but also by a corresponding increase in the optical density

of the path that photons must transverse, an increase in the number of absorbed photons, and the corresponding reduction of detection sensitivity. Another contributing factor to the negative slope of the graph is that, generally, as tumors grow the capacity of the imperfect tumor capillary system to irrigate the interior decreases, reducing the supply of luciferin and oxygen and lowering light production.

The combined use of noninvasive ICCD video imaging and luminometric analysis of tumor homogenates provides continuous monitoring of spatial changes and sensitive quantification of tumor growth and should facilitate both basic research and the evaluation of new therapies.

Materials and Methods

Cells and Cell Culture

PC-3, LNCaP, and DU 145 cells were purchased from the American Type Culture Collection (Rockville, Maryland) and maintained in a 1:1 mixture of DMEM and Ham's nutrient mixture F12, supplemented with 10% fetal bovine serum (FBS). PC-3.Sluc, LNCaP.Sluc, and DU 145.Sluc cell sublines were generated by transfection of the corresponding cell lines with the pRC/CMV expression vector (Invitrogen, San Diego, California), containing the firefly (*Photinus pyralis*) luciferase gene coding region, and cloned as described (Rubio et al, 1998).

Luciferase Assay

Luciferase activity in cell or tissue extracts was measured by chemiluminescence, using the standard luciferase assay kit (Promega Corporation, Madison, Wisconsin). Production of light was measured using a Turner Designs luminometer model TD 20/20, after addition of 100 μ l of luciferase assay reagent (Promega Corporation) to 20 μ l of cell lysate or tissue homogenate. Light detector measurements are expressed in RLUs.

Cell and Tissue Homogenates

Cell lysates were prepared by performing one freeze-thaw cycle in Reporter lysis buffer (RLB) (Promega Corporation). Whole organ and tumor tissue extracts were prepared by mechanical homogenization of tissue in RLB at a 1/1 ratio (weight/volume), using an Ultra-Turrax T-25 tissue homogenizer (Janke and Kunkel, Staufen, Germany) followed by centrifugation at 25,000 $\times g$ for 45 minutes and 4 $^{\circ}$ C to remove insoluble particles. In the case of lymph nodes, tissue homogenates were made in the presence of 10% BSA, as a protection against proteases.

Number of RLUs Per Cell

Standard curves were generated using a luminometer to measure light production from known quantities of tumor cells, in RLB homogenates (Rubio et al, 2000).

Counting of TCEs and Detection Sensitivity

TCEs is a magnitude equal to the total amount of light detected, by the luminometer, divided by the amount of light generated by a single cell in culture. This convention was adopted for practical reasons because it provides an approximated idea of the number of tumor cells present in the tissue homogenates.

To calculate the number of TCEs present in mice tissues, the corresponding background light was subtracted from the RLUs produced by a 20- μ l aliquot of tissue homogenate and the resulting number was then divided by the slope of the standard curve, generated in the corresponding tissue homogenate. Tissue homogenates in which the luciferase activity of a 20- μ l aliquot exceeded detector range capacity (9999 RLU/min) were adapted to the counter range by diluting with RLB. Assay sensitivity was defined as the number of TCEs required to generate a quantity of light equivalent to two standard deviations of the background chemiluminescence.

Experimental Tumors and Tumor Growth

Six-week-old BALB/c homozygous nude (nu/nu) mice were purchased from IFFA-CREDO (L'Arbresle, France) and maintained in a specific pathogen-free environment throughout the experiment. To generate intramuscular tumors, animals were inoculated in each thigh with 10^6 luciferase-expressing tumor cells, suspended in 100 μ l of culture media without FBS, and killed at the indicated times. To generate orthotopic tumors, animals were inoculated in each prostate lobe with 5×10^5 luciferase-expressing tumors cells, suspended in 50 μ l of culture media without FBS, as described (Stephenson et al, 1992). Necropsies were performed and primary tumors and organs of interest harvested.

For cytostatic treatment, mice were inoculated ip daily with 10 mg/kg paclitaxel (Bristol-Myers Squibb, New York, New York) in 0.9% w/v NaCl solution. Control animals were inoculated with 0.9% w/v NaCl solution instead of paclitaxel.

Image Capture and Processing

Mice were anesthetized with a mixture of droperidol (Roche, Basel, Switzerland) 6 mg/kg and midazolam (Rovi S.A., Madrid, Spain) 12 mg/kg and then inoculated ip with 150 μ l of an aqueous solution of luciferin 100 mg/kg. For image capture, the animals were immobilized by fixing the extremities with opaque insulating tape and placed at either a 10- or 35-cm distance from the camera objective, inside an optically insulated chamber. For close-up images of chest and pelvis, opaque insulating tape was used to cover the primary tumor areas and avoid saturation of the detection device by excess photons. Images were acquired during a 4-minute period, routinely starting 4 minutes after luciferin administration, using an ICCD video camera (VIM Camera C 2400-32; effective number of pixels 756(H) \times 485(V), cell size 8.4(H) \times 9.8(V) μ m) fitted with an Argus 20 image processor and a

personal computer (Hamamatsu Photonics, Hamamatsu City, Japan). Immediately after image acquisition, while the animal remained in the same position, a second black and white image of the animal surface was obtained using ambient light.

To determine the detection sensitivity of tumor cells in culture, triplicate serial dilutions from 70 to 0 PC-3.Sluc cells were plated in 96-well microtiter tissue culture plates and imaged after luciferin. Luciferase photon images were color coded using magenta, blue, green, yellow, and red, in this order, to indicate increasing light intensities.

Color coding, superposition of luciferase photon images, and ambient light images was done using the Photoshop (Adobe Systems, Mountain View, California) image processing program. Quantification of image-recorded photons events was done using the Image Pro Plus software (Media Cybernetics, Silver Spring, Maryland). The V shape of the close-up pelvic images resulted from having covered the thighs with opaque masking tape to shield the camera from light emitted by the tumors, which at close range would have otherwise saturated the ICCD.

Acknowledgements

We thank Ms. Maria Dolores Gomez and Mr. Eugenio Grau of Instituto de Biologia Molecular y Celular de Plantas, CSIC, Valencia, for advice and help in the use of the ICCD video equipment.

References

- Benaron DA, Cheong WF, and Stevenson DK (1997). Tissue optics. *Science* 276:2002–2003.
- Blagosklonny MV, Dixon SC, and Figg WD (2000). Efficacy of microtubule-active drugs followed by ketoconazole in human metastatic prostate cancer cell lines. *J Urol* 163:1022–1026.
- Brandes C, Plautz JD, Stanewsky R, Jamison CF, Straume M, Wood KV, Kay SA, and Hall JC (1996). Novel features of drosophila period Transcription revealed by real-time luciferase reporting. *Neuron* 16:687–692.
- Campbell A and Sala-Newby G (1996). Bioluminescent and chemiluminescent indicators for molecular signaling and function in living cells. In: Mason WT, editor. *Fluorescent and luminescent probes for biological activity*. New York: Academic Press, 58–82.
- Contag CH, Spilman SD, Contag PR, Oshiro M, Eames B, Dennery P, Stevenson DK, and Benaron DA (1997). Visualizing gene expression in living mammals using a bioluminescent reporter. *Photochem Photobiol* 66:523–531.
- De Brabander M, Geuens G, Nuydens R, Willebrords R, and De Mey J (1982). Microtubule stability and assembly in living cells: The influence of metabolic inhibitors, taxol and pH. *Cold Spring Harb Symp Quant Biol* 46:227–240.
- Horoszewicz JS, Leong SS, Kawinski E, Karr JP, Rosenthal H, Chu TM, Mirand EA, and Murphy GP (1983). LNCaP model of human prostatic carcinoma. *Cancer Res* 43:1809–1818.
- Horwitz SB, Parness J, Schiff PB, and Manfredi JJ (1982). Taxol: A new probe for studying the structure and function of microtubules. *Cold Spring Harb Symp Quant Biol* 46:219–226.

- Kaighn ME, Narayan KS, Ohnuki Y, Lechner JF, and Jones LW (1979). Establishment and characterization of a human prostatic carcinoma cell line (PC-3). *Invest Urol* 17:16–23.
- Kay SA (1993). Shedding light on clock controlled cab gene transcription in higher plants. *Semin Cell Biol* 4:81–86.
- Mahler C and Denis L (1992). Management of relapsing disease in prostate cancer. *Cancer* 70:329–334.
- Matsumoto K, Anzai M, Nakagata N, Takahashi A, Takahashi Y, and Miyata K (1994). Onset of paternal gene activation in early mouse embryos fertilized with transgenic mouse sperm. *Mol Reprod Dev* 39:136–140.
- Mickey DD, Stone KR, Wunderli H, Mickey GH, Vollmer RT, and Paulson DF (1977). Heterotransplantation of a human prostatic adenocarcinoma cell line in nude mice. *Cancer Res* 37:4049–4058.
- Millar AJ, Carre IA, Strayer CA, Chua NH, and Kay SA (1995). Circadian clock mutants in *Arabidopsis* identified by luciferase imaging. *Science* 267:1161–1163.
- Millar AJ, Short SR, Chua NH, and Kay SA (1992). A novel circadian phenotype based on firefly luciferase expression in transgenic plants. *Plant Cell* 4:1075–1087.
- Müller G, Chance B, and Alfano R, editors. (1993). *Medical optical tomography: Functional imaging and monitoring*. Bellingham, WA: SPIE Press Optical Engineering Press.
- Pettaway CA, Pathak S, Greene G, Ramirez E, Wilson MR, Killion JJ, and Fidler IJ (1996). Selection of highly metastatic variants of different human prostatic carcinomas using orthotopic implantation in nude mice. *Clin Cancer Res* 2:1627–1636.
- Rubio N, Villacampa MM, and Blanco J (1998). Traffic to lymph nodes of PC-3 prostate tumor cells in nude mice visualized using the luciferase gene as a tumor cell marker. *Lab Invest* 78:1315–1325.
- Rubio N, Villacampa MM, El Hilali N, and Blanco J (2000). Metastatic burden in nude mice organs measured using prostate tumor PC-3 cells expressing the luciferase gene as a quantifiable tumor cell marker. *Prostate* 44:133–143.
- Stephenson RA, Dinney CP, Gohji K, Ordenez NG, Killion JJ, and Fidler IJ (1992). Metastatic model for human prostate cancer using orthotopic implantation in nude mice. *J Natl Cancer Inst* 84:951–957.
- Sweeney TJ, Mailander V, Tucker AA, Olomu AB, Zhang W, Cao Y, Negrin RS, and Contag CH (1999). Visualizing the kinetics of tumor-cell clearance in living animals. *Proc Natl Acad Sci USA* 96:12044–12049.
- Tamiya E, Sugiyama T, Masaki K, Hirose A, Okoshi T, and Karube I (1990). Spatial imaging of luciferase gene expression in transgenic fish. *Nucleic Acids Res* 18:1072–1076.
- Thalmann GN, Anezinis PE, Chang SM, Zhou HE, Kim EE, Hopwood VL, Pathak S, von Eschenbach AC, and Chung LW (1994). Androgen-independent cancer progression and bone metastasis in the LNCaP model of human prostate cancer. *Cancer Res* 54:2577–2581.
- Thompson EM, Adenot P, Tsuji FI, and Renard JP (1995). Real time imaging of transcriptional activity in live mouse preimplantation embryos using a secreted luciferase. *Proc Natl Acad Sci USA* 92:1317–1321.
- Webber MM, Bello D, and Quader S (1997). Immortalized and tumorigenic adult human prostatic epithelial cell lines: Characteristics and applications. Part 2. Tumorigenic cell lines. *Prostate* 30:58–64.
- Weissleder R, Tung CH, Mahmood U, and Bogdanov A (1999). In vivo imaging of tumors with protease-activated near-infrared fluorescent probes. *Nat Biotechnol* 17:375–378.
- Yang M, Baranov E, Jiang P, Sun FX, Li XM, Li L, Hasegawa S, Bouvet M, Al-Tuwaijri M, Chishima T, Shimada H, Moossa AR, Penman S, and Hoffman RM (2000). Whole-body optical imaging of green fluorescent protein-expressing tumors and metastases. *Proc Natl Acad Sci USA* 97:1206–1211.
- Yang M, Jiang P, Sun FX, Hasegawa S, Baranov E, Chishima T, Shimada H, Moossa AR, and Hoffman RM (1999). A fluorescent orthotopic bone metastasis model of human prostate cancer. *Cancer Res* 59:781–786.